Issartel, J.-P., Lunardi, J., & Vignais, P. V. (1986) *J. Biol. Chem. 261*, 895–901.
Issartel, J.-P., Favre-Bulle, O., Lunardi, J., & Vignais, P. V. (1987) *J. Biol. Chem. 262*, 13538–13544.
Kalashnikova, T. Y., Milgrom, Y. M., & Murataliev, M. B. (1988) *Eur. J. Biochem. 177*, 213–218.
Kironde, F. A. S., & Cross, R. L. (1986) *J. Biol. Chem. 261*, 12544–12549.
Klein, G., Satre, M., Zaccaï, G., & Vignais, P. V. (1982) *Biochim. Biophys. Acta 681*, 226–232.
Knowles, A. F., & Penefsky, H. S. (1972) *J. Biol. Chem. 247*, 6617–6623.
Larson, E. M., & Jagendorf, A. T. (1989) *Biochim. Biophys. Acta 973*, 67–77.
Lauquin, G., Pougeois, R., & Vignais, P. V. (1980) *Biochemistry 19*, 4620–4626.
Lundin, A., Rickardson, A., & Thore, A. (1976) *Anal. Biochem. 75*, 611–620.
Penefsky, H. S. (1977) *J. Biol. Chem. 252*, 2891–2899.
Penin, F., Godinot, C., & Gautheron, D. C. (1984) *Biochim. Biophys. Acta 775*, 239–245.
Senior, A. E. (1988) *Physiol. Rev. 68*, 177–231.
Vignais, P. V., & Lunardi, J. (1985) *Annu. Rev. Biochem. 54*, 977–1014.
Walker, J. E., Fearnley, I. M., Gay, N. J., Gibson, B. W., Northrop, F. D., Powell, S. J., Runswick, M. J., Saraste, M., & Tybulewicz, V. L. J. (1985) *J. Mol. Biol. 184*, 677–701.

Substitution of Amino Acids in Helix F of Bacteriorhodopsin: Effects on the Photochemical Cycle†

Patrick L. Ahl,‡,§ Lawrence J. Stern,∥,⊥ Tatsushi Mogi,∥,# H. Gobind Khorana,∥ and Kenneth J. Rothschild*,‡

Departments of Physics and Physiology, Boston University, 590 Commonwealth Avenue, Boston, Massachusetts 02215, and Departments of Biology and Chemistry, Massachusetts Institute of Technology, Cambridge, Massachusetts 02139

Received April 18, 1989; Revised Manuscript Received July 21, 1989

ABSTRACT: The effects of amino acid substitutions in helix F of bacteriorhodopsin on the photocycle of this light-driven proton pump were studied. The photocycles of Ser-183→Ala and Glu-194→Gln mutants were qualitatively similar to that of wild-type bacteriorhodopsin produced in *Escherichia coli* and bacteriorhodopsin from *Halobacterium halobium*. The substitution of a Phe for either Trp-182 or Trp-189 significantly reduced the fraction of photocycling bacteriorhodopsin. The amino acid substitutions Tyr-185→Phe and Ser-193→Ala substantially increased the lifetime of the photocycle without substantially increasing the lifetime of the M photocycle intermediate. Similar results were also obtained with the Pro-186→Gly substitution. In contrast, replacing Pro-186 with the larger residue Leu inhibited the formation of the M photocycle intermediate. These results are consistent with a structural model of the retinal-binding pocket suggested by low-temperature UV/visible and Fourier transform infrared difference spectroscopies that has Trp-182, Tyr-185, Pro-186, and Trp-189 forming part of the binding pocket.

Bacteriorhodopsin (bR)[1] is a light-driven proton pump in the purple membrane of *Halobacterium halobium*. The amino acid sequence contains seven hydrophobic regions labeled A–G that correspond to the seven transmembrane helices[2] (Henderson & Unwin, 1975; Khorana et al., 1979; Ovchinnikov et al., 1979; Huang et al., 1982). The chromophore, *all-trans*-retinal, is covalently linked to Lys-216 in helix G through a protonated Schiff base (Bayley et al., 1981; Katre et al., 1981; Rothschild et al., 1982). Light absorption by retinal initiates the bR photocycle by causing isomerization about the 13–14 double bond (Braiman & Mathies, 1982). The photocycle, which occurs on a millisecond time scale at room temperature, involves at least five intermediates:[3] $BR_{568} \rightarrow K_{610} \rightarrow L_{550} \rightarrow M_{412} \rightarrow O_{640} \rightarrow BR_{568}$ (Lozier et al., 1975). There is also considerable evidence for a sixth intermediate, N, between M and O which has a λ_{max} near 550 nm (Dancsházy et al., 1988; Kouyama et al., 1988; Nagle et al., 1982; Xie et al., 1987).

Site-directed mutagenesis can be used to examine the role of individual amino acids in the structure and function of

† Supported by grants from the National Science Foundation (DMB-8806007) and the Office of Naval Research (N00014-88-04164) to K.J.R.; grants from the National Science Foundation (PCM-8110992), National Institutes of Health (GM28289-06 and AI-11479), and Office of Naval Research, Department of the Navy (N00014-82-K-0668) to H.G.K.; and a postdoctoral fellowship from American Heart Association Massachusetts Affiliate to P.L.A. L.J.S. is a NIH predoctoral trainee.

* To whom correspondence should be addressed at the Department of Physics, Boston University, 590 Commonwealth Ave., Boston, MA 02215.
‡ Boston University.
§ Present address: Department of Pathology and Laboratory Medicine, Hahnemann University, Philadelphia, PA 19102.
∥ Massachusetts Institute of Technology.
⊥ Present address: Departments of Biochemistry and Molecular Biology, Harvard University, Cambridge, MA 02138.
Present address: Department of Biology, Faculty of Science, University of Tokyo, Hongo, Tokyo 113, Japan.

[1] Abbreviations: AU, absorbance unit; bR, bacteriorhodopsin; FTIR, Fourier transform infrared; ebR, bacteriorhodopsin produced in *E. coli*; PM, purple membrane; W182F, Trp-182→Phe; S183A, Ser-183→Ala; Y185F, Tyr-185→Phe; P186G, Pro-186→Gly; P186L, Pro-186→Leu; W189F, Trp-189→Phe; S193A, Ser-193→Ala; E194Q, Glu-194→Gln.

[2] Amino acids in the putative bR helices A–G are based on the folding model proposed by Huang et al. (1982).

[3] BR designates the light-adapted state of bacteriorhodopsin. The subscripts indicate the λ_{max} of the photocycle intermediates. The wavelength subscript designations for BR and the photocycle intermediates are not used throughout the rest of this paper since the λ_{max} values vary for many of the mutants [see Ahl et al. (1988)].

0006-2960/89/0428-10028$01.50/0

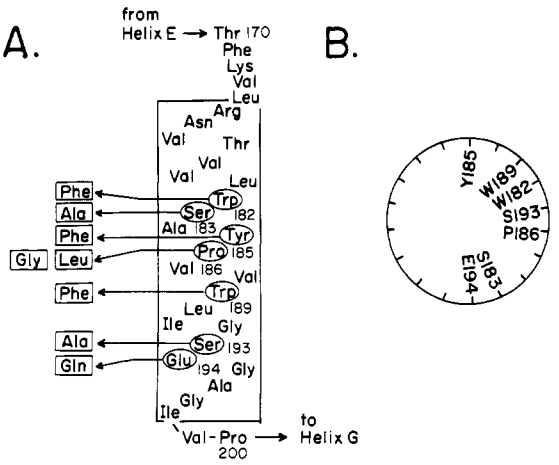

FIGURE 1: (A) Putative helix F of bacteriorhodopsin. Eight single amino acid substitutions were made in helix F. Two separate amino acid substitutions were made at position 186. The retinal is attached via a Schiff base at Lys-216 in helix G. (B) Helical wheel projection plot of the amino acids in helix F substituted by site-specific mutagenesis.

proteins (Ackers & Smith, 1985; Knowles, 1987). In this paper, we have examined the effects of eight amino acid substitutions in helix F (Figure 1) on the bR photocycle kinetics. This region of the protein was chosen because cross-linking studies with a photoaffinity retinal analogue indicate that the β-ionone ring of the chromophore is located near residues Ser-193 and Glu-194 which are in helix F (Huang et al., 1982). In addition, amino acid side chains with hydrogen-bonding groups might be part of a proton-conducting hydrogen-bond network, i.e., a proton wire (Nagle & Morowitz, 1978). To test for this possibility, amino acid replacements were chosen to substitute hydrogen-bonding groups in the side chains for non-hydrogen-bonding groups with a minimum alteration in the shape of the side chain. Thus, Ser-183 and Ser-193 were changed to Ala, Trp-182, Trp-189, and Tyr-185 were changed to Phe, and Glu-194 was changed to Gln. Pro-186 was changed to Leu and to Gly. A helical wheel projection map of the helix F indicates that Trp-182, Tyr-185, Pro-186, Trp-189, and Ser-193 are within a 100° segment of the putative α-helix (see Figure 1).

All of the bR mutants examined pump protons in response to illumination, although the initial rate and steady-state level of pumping activity were significantly reduced for P186L (Hackett et al., 1987; Mogi et al., 1987, 1989a,b). We have previously reported the room temperature absorption spectra together with the low-temperature UV/visible difference spectra of the K and M intermediates for these mutants (Ahl et al., 1988). These experiments indicated that Trp-182, Tyr-185, Pro-186, Trp-189, and possibly Ser-193 form part of the retinal-binding pocket. The effects of these amino acid substitutions on the room temperature photocycle kinetics are consistent with this conclusion. Substitutions at Ser-183 and Glu-194, which are believed to be directed away from the binding site, had relatively minor effects on the photocycle kinetics compared with the other substitutions.

Experimental Methods

Isolation and Reconstitution of Escherichia coli Produced Bacteriorhodopsin. The construction of the bacteriorhodopsin genes for these mutants and their expression in *E. coli* have been described (Lo et al., 1984; Hackett et al., 1987; Mogi et al., 1989a). Bacteriorhodopsin was purified from *E. coli* membranes by organic solvent extraction and by gel filtration and ion-exchange chromatographies (Braiman et al., 1987). The samples were prepared by reconstitution of the purified apoproteins with polar lipids from *H. halobium* (Bayley et al., 1982) and *all-trans*-retinal followed by dialysis to produce small unilamellar vesicles according to the procedure of Popot et al. (1986). Control samples were reconstituted in an identical manner by using the wild-type protein produced in *E. coli* (ebR). This reconstitution procedure produced membranes with a high protein to lipid ratio that have a lattice similar to the purple membrane (PM) when subject to partial drying (Trewhella et al., 1986). Purple membrane was isolated from *H. halobium* strain ET1001 following standard procedures (Oesterhelt & Stoeckenius, 1974).

The samples were suspended in 0.15 M KCl, 0.05 M potassium phosphate, and 0.025% NaN_3, pH 6.0. The protein concentration was 80–100 μM. The absorption spectra of both P186G and P186L are salt dependent (Ahl et al., 1988; Mogi et al., 1989a). At 150 mM KCl the λ_{max} values of both these mutants were significantly blue shifted relative to ebR and the rest of the helix F mutants. In contrast, at 2 M NaCl the λ_{max} of P186G shifted to around 570 nm, and P186L had a strong absorbance shoulder at 560 nm. Since the λ_{max} values of both P186G and P186L at 2 M NaCl were the most similar to that of wild-type bR, these mutants were also examined in 2 M NaCl, 0.15 M KCl, 0.05 M potassium phosphate, and 0.025% NaN_3, pH 6.0.

Flash Spectroscopy. The photocycle transient absorbance changes were recorded by using a laser flash photolysis apparatus of our own design. About 15 μL of sample at 80–100 μM protein was sealed in a 1 mm × 1 mm (i.d.) glass capillary tube (Vitro Dynamics, Inc., Rockaway, NJ). The capillary tube was mounted on a temperature-controlled copper sample stage. The temperature was controlled by a Peltier heating/cooling unit (Bailey Instruments, Saddle Brook, NJ). The measuring light source was a 50-W quartz halogen lamp (Model 6332, Oriel Corp., Stamford, CT) that was focused on a monochromator (Model 82-410, Jarrel-Ash, Acton, MA) which selected the measuring wavelength. The actinic flash was from a dye laser of our own design which was pumped by a 250-kW N_2 pulse laser (Model UV-12, Cooper LaserSonics, Inc., Santa Clara, CA). The laser dye was coumarin 540A (Exciton Chemical Co., Inc., Dayton, OH). The actinic flash energy was 0.2–0.3 mJ/flash, and the flash duration was about 10 ns. The actinic flash was oriented 90° relative to the measuring light path and was focused down at the sample to approximately a 1.5-mm radius circle. The measuring light intensity was detected by a red sensitive photomultiplier (Model 9846B, Thorn EMI Gencom, Inc., Plainview, NY) using a 1 kΩ load resistor. Narrow bandwidth interference filters (Ditric Optics, Inc., Hudson, MA) were used to block the scattered actinic flash light from the photomultiplier.

The voltage from the photomultiplier load resistor was amplified by a 1-MHz differential amplifier (Model 5A22N, Textronix, Inc., Beaverton, OR). The signal was then digitized and stored in a microcomputer (Model 1275, Nicolet Analytical Instruments, Madison, WI). The voltage change, which is proportional to the light intensity change [$\Delta I(t)$], together with the voltage proportional to the measuring light intensity (I) was recorded. The voltage proportional to the light intensity (I_0) at 570 nm when the sample was removed from the measuring light path was recorded. The 570-nm absorbance of each sample was calculated by using I and I_0 at 570 nm. To improve the signal to noise ratios 1000–4000 scans were signal averaged. The triggering of the actinic flash and the microcomputer was done with a waveform generator (Model FG 501A, Textronix) and a time delay generator (Model 7010,

Table I: Photocycle Parameters for 21–23 °C

	570 nm				410 nm			
	ΔA_{570}[a]	τ_f[b] (f_f)[c]	τ_s[b] (f_s)[c]	τ_{570}[d]	ΔA_{410}[a]	τ_f[b] (f_f)[c]	τ_s[b] (f_s)[c]	τ_{410}[d]
controls[e]								
PM	−0.110		5.7 (1.00)	5.7	0.044		7.9 (1.00)	7.9
ebR	−0.061	4.3 (0.85)	19 (0.14)	6.3	0.031		4.8 (1.00)	4.8
group A								
Ser-183→Ala	−0.052	2.4 (0.41)	9.0 (0.57)	6.1	0.021	1.0 (0.55)	4.5 (0.45)	2.6
Glu-194→Gln	−0.051	1.0 (0.19)	13 (0.81)	11	0.019	2.4 (0.41)	11 (0.59)	7.6
group B								
Trp-182→Phe	−0.009	2.5 (0.89)	16 (0.11)	4.0	0.003		3.6 (1.00)	3.6
Trp-189→Phe	−0.006		15 (1.00)	15	0.004		7.3 (1.00)	7.3
group C								
Tyr-185→Phe	−0.032	5.5 (0.18)	107 (0.82)	89	0.004		17 (1.00)	17
Ser-193→Ala	−0.012	16 (0.37)	74 (0.63)	53	0.004		8.7 (1.00)	8.7

[a] ΔA_{570} and ΔA_{410}, maximum absorbance change at 570 and 410 nm, respectively in absorbance units. [b] τ, relaxation time of the fast, τ_f, or slow, τ_s, component in milliseconds. If the decay was best fit by a single exponential, then the relaxation time is defined as τ_s. [c] f, fraction of total absorbance change of either the fast, f_f, or slow, f_s, component. [d] τ_{570} and τ_{410}, average relaxation time at 570 and 410 nm, respectively, where $\tau_{av} = \tau_f f_f + \tau_s f_s$. [e] The measurements were made at the following temperatures: PM, 23 °C; ebR, 22 °C; S183A, 25 °C; E194Q, 22 °C; W182F, 23 °C; W189F, 22 °C; Y185F, 21 °C; S193A, 21 °C.

Table II: Photocycle Parameters for 30–32 °C

	570 nm				410 nm			
	ΔA_{570}	τ_f (f_f)	τ_s (f_s)	τ_{570}	ΔA_{410}	τ_f (f_f)	τ_s (f_s)	τ_{410}
controls[a]								
PM	−0.094		2.9 (1.00)	2.9	0.039	1.7 (0.81)	4.4 (0.18)	2.2
ebR	−0.040	<0.5[b] (0.52)	6.1 (0.48)	3.2	0.013	3.2 (0.80)	11 (0.20)	4.8
group A								
Ser-183→Ala	−0.043	0.92 (0.36)	5.0 (0.62)	3.4	0.019	0.77 (0.55)	3.2 (0.44)	1.8
Glu-194→Gln	−0.031	1.7 (0.24)	8.4 (0.74)	6.6	0.011		5.1 (1.00)	5.1
group B								
Trp-182→Phe	−0.012	0.5 (0.74)	4.5 (0.24)	1.4	0.002		1.9 (1.00)	1.9
Trp-189→Phe	−0.004		7.4 (1.00)	7.4	0.003		3.6 (1.00)	3.6
group C								
Tyr-185→Phe	−0.023	39 (0.75)	165 (0.25)	71	0.004		14 (1.00)	14
Ser-193→Ala	−0.013	10 (0.61)	49 (0.38)	25	0.004		6.0 (1.00)	6.0

[a] The measurements were made at the following temperatures: PM, 31 °C; ebR, 30 °C; S183A, 32 °C; E194Q, 31 °C; W182F, 30 °C; W189F, 31 °C; Y185F, 30 °C; S193A, 30 °C. [b] The computer program was not able to accurately determine this relaxation time, which was less than 0.5 ms.

Table III: Photocycle Parameters for the Pro-186 Mutants

	570 nm				410 nm			
	ΔA_{570}	τ_f (f_f)	τ_s (f_s)	τ_{570}	ΔA_{410}	τ_f (f_f)	τ_s (f_s)	τ_{410}
group D[a]								
2 M NaCl								
Pro-186→Gly	−0.027	8.5 (0.62)	209 (0.38)	85	0.006		5.8 (1.00)	5.8
Pro-186→Leu	−0.010	6.7 (0.55)	40 (0.45)	22	0.001		2.1 (1.00)	2.1
150 mM KCl								
Pro-186→Gly	−0.039	5.2 (0.70)	118 (0.30)	39	0.011		2.1 (1.00)	2.1
Pro-186→Leu	−0.014	5.3 (0.49)	244 (0.51)	127				

[a] The measurements were made at the following temperatures: in 2 M NaCl, P186G and P186L, 22 °C; in 150 mM KCl, P186G, 21 °C, and P186L, 22 °C.

Berkeley Nucleonics Corp., Berkeley, CA). The flash repetition rate was set at 2 Hz.

Data Analysis. The light-intensity changes as a function of time were converted to absorbance changes [$\Delta A(t)$] by using

$$\Delta A(t) = -\log [(\Delta I(t)/I) + 1]$$

The time-dependent absorbance changes were fit to a multiexponential decay model as described in the accompanying paper (Stern et al., 1989) by using a nonlinear least-squares fitting program (program 360D13.6003, Triangle Universities Computation Center, Research Triangle Park, NC). The ratio of the χ^2 for the absorbance change to the χ^2 for the pre-flash base line was used to calculate the reduced χ^2 of the fit (Bevington, 1969). The transient absorbance change decays at 570 and 410 nm were generally well fit by either the one- or two-exponential model.

Results

In the following section, the mutants have been separated into four groups on the basis of similar photocycle characteristics. The amplitudes (ΔA_{570} and ΔA_{410}) and the fast and slow relaxation times (τ_f and τ_s) of the absorbance changes for each of the samples were determined by fitting to either a one- or two-exponential decay model. Tables I and II show these photocycle parameters in the 21–25 and 30–32 °C temperature ranges, respectively, for all the mutants except P186G and P186L. The photocycle parameters for the Pro-186 mutants are listed in Table III for only the room temperature case. The fraction of the total absorbance change for each decay component is shown in parentheses. Parameters τ_{570} and τ_{410} are the weighted averages of the fast and slow decay components for the 570- and 410-nm absorbance change, respectively.

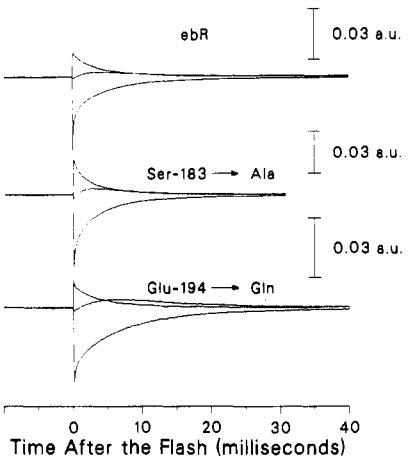

FIGURE 2: Absorbance changes for ebR, S183A, and E194Q. Absorbance changes at 570, 410, and 640 nm are shown for ebR (0.58), S183A (0.41), and E194Q (0.43) for 30–32 °C. The absorbance of each sample at 570 nm is shown in parentheses. For each record set the negative absorbance change is the 570-nm record, the positive absorbance change is the 410-nm record, and the 640-nm record is the small positive absorbance change located between the 570- and 410-nm absorbance changes. All the record sets are displayed on the same time scale, which is shown at the bottom, while the absorbance scales for each record set are indicated by the vertical scale bar to the right of each record.

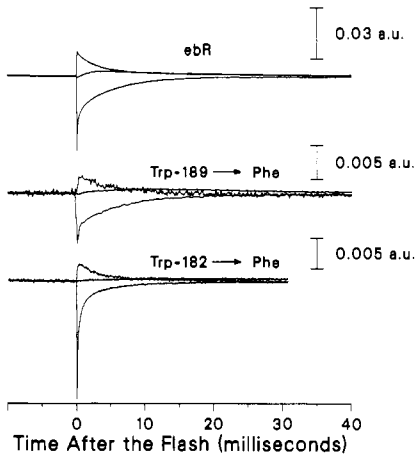

FIGURE 3: Absorbance changes for ebR, W189F, and W182F. Absorbance changes at 570, 410, and 640 nm are shown for ebR (0.58), W189F (0.42), and W182F (0.79) for 30–32 °C. The absorbance of each sample at 570 nm is shown in parentheses. For each record set the large negative absorbance change is the 570-nm record, the large positive absorbance change is at 410 nm, and the small absorbance change is at 640 nm. The absorbance scales for W189F and W182F are 6-fold smaller than the ebR scale as indicated by the vertical scale bars to the right of each record.

ebR. The top record of Figure 2 shows the transient absorbance changes at 570, 410, and 640 nm for membranes containing ebR. The transient absorbance decrease at 570 nm is due to the depletion of the BR state; the positive absorbance changes at 410 and 640 nm are due to the formation and decay of the M and O intermediates, respectively. As shown in Tables I and II the amplitudes and relaxation times for the absorbance changes of ebR were similar to those of PM.

Ser-183→Ala and Glu-194→Gln. The flash-induced absorbance changes for S183A and E194Q were qualitatively the most similar to that for ebR (Figure 2). The M intermediate decay of these mutants was only slightly faster than the return of the BR state measured at 570 nm. The positive absorbance change at 640 nm indicates an O intermediate was formed at this pH. As shown in Tables I and II, the photocycle amplitudes and relaxation times of S183A and E194Q (group A) were the most similar to the corresponding parameters of the control samples, i.e., ebR and PM. The Glu-194→Gln substitution appeared to slow the photocycle slightly more than the Ser-183→Ala substitution. This suggests that Glu-194 may have a relatively small or indirect effect on the photocycle. However, compared to the other mutations we examined in helix F, the perturbations produced by S183A and E194Q were relatively minor.

Trp-182→Phe and Trp-189→Phe. The typical absorbance changes for the Trp mutants W182F and W189F (group B) are shown in Figure 3 together with the ebR record set for comparison. Although the photocycle relaxation times for the Trp mutants were similar to that for ebR, the amplitudes of the absorbance changes were significantly smaller. Since the bleaching flash energy was approximately the same for all samples, this cannot account for the reduction in the amplitude of the photocycle. Both W182F and W189F had a small positive absorbance change at 640 nm, indicating that a photocycle intermediate similar to the O intermediate was formed. The 570-nm absorbance decay was well fit by a single exponential for W189F, while for W182F the 570-nm absorbance change was clearly better fit by two exponentials (see Tables I and II).

Tyr-185→Phe and Ser-193→Ala. The absorbance changes

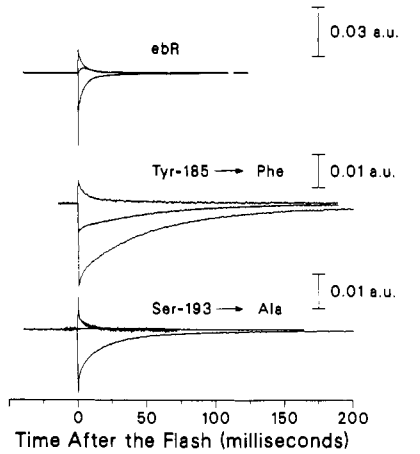

FIGURE 4: Absorbance changes for ebR, Y185F, and S193A. Absorbance changes at 570, 410, and 640 nm are shown for ebR (0.58), Y185F (0.62), and S193A (0.46) for 30–32 °C. The absorbance of each sample at 570 nm is shown in parentheses. The identification of the records for each measuring wavelength is the same as in Figures 1 and 2.

for Y185F and S193A (group C) are shown along with the ebR record set in Figure 4. Both Y185F and S193A substantially increased the lifetime of the 570-nm absorbance change compared to the ebR control. However, these substitutions did not produce a comparable increase in the lifetime of the 410-nm absorbance change. For example, the room temperature average relaxation time at 570 nm (τ_{570}) for Y185F was 14-fold greater than the corresponding relaxation time for ebR, while the corresponding increase in the average relaxation time at 410 nm (τ_{410}) was only 3.5-fold. This indicates that the close connection between M intermediate decay and the lifetime of the photocycle was altered by these amino acid substitutions.

The Y185F and S193A substitutions also reduced the amplitude of the photocycle signal, however, not as much as W182F and W189F. The temperature dependence of these mutant photocycles was also different from that of the rest of the mutants. Both Y185F and S193A exhibited a shift in the relative amplitudes of the fast and slow relaxation times at the warmer temperatures (see Tables I and II). There were,

Table IV: Comparison of General Photocycle Characteristics

	21–25 °C			30–32 °C		
	$-\Delta A_{570}/A_{570}$[a]	$-\Delta A_{410}/\Delta A_{570}$	τ_{570}/τ_{410}	$-\Delta A_{570}/A_{570}$	$-\Delta A_{410}/\Delta A_{570}$	τ_{570}/τ_{410}
controls						
PM	0.20	0.40	0.72	0.17	0.41	1.3
ebR	0.11	0.52	1.3	0.07	0.33	0.67
group A						
Ser-183→Ala	0.12	0.40	2.3	0.10	0.44	1.9
Glu-194→Gln	0.12	0.37	1.4	0.07	0.34	1.3
group B						
Trp-182→Phe	0.01	0.33	1.1	0.02	0.15	0.74
Trp-189→Phe	0.01	0.66	2.0	0.01	0.75	2.0
group C						
Tyr-185→Phe	0.05	0.13	5.2	0.04	0.17	5.0
Ser-193→Ala	0.03	0.33	6.0	0.03	0.31	4.1
group D						
2 M NaCl						
Pro-186→Gly	0.05	0.22	15			
Pro-186→Leu	0.02	0.10	10			
150 mM KCl						
Pro-186→Gly	0.06	0.28	19			
Pro-186→Leu	0.19	0.00	no M formed			

[a] A_{570}, the sample absorbance at 570 nm.

however, clear differences between the photocycles of Y185F and S193A. A small positive absorbance change at 640 nm, consistent with O intermediate formation, was observed for S193A in the 30–32 °C range, while the 640-nm transient absorbance change for Y185F was negative, indicating little if any O intermediate was formed (see Figure 4). However, we observed that the negative 640-nm absorbance change for Y185F at this pH was significantly reduced in room temperature experiments.

Pro-186→Leu and Pro-186→Gly. The largest alterations to the room temperature photocycle were produced by substitutions at Pro-186 (Figure 5 and Table III). Substitution of a Leu at Pro-186 almost completely abolished, as measured at 410 nm, formation of the M intermediate in 0.15 M KCl. Absorbance changes in 0.15 M KCl were also monitored at 380, 400, and 420 nm for P186L. Again, no positive absorbance changes were observed. Thus, the formation of the M intermediate is almost completely inhibited for P186L in 0.15 M KCl. However, in 2 M NaCl a small positive 410-nm absorbance change was detected. As shown in Figure 5, the M intermediate amplitude for P186L in 2 M NaCl was significantly reduced relative to the 570-nm absorbance change.

Only a small reduction in relative amplitude of the 410-nm absorbance change was found for the 0.15 M KCl form of P186G. This indicates that the Pro-186→Gly substitution did not inhibit M intermediate formation as did the Pro-186→Leu substitution (see Table III). The λ_{max} of P186G at 2 M NaCl is similar to that of ebR, while at 0.15 M KCl the λ_{max} is near 470 nm (Mogi et al., 1989a). Although the λ_{max} of the 2 M NaCl form of P186G is similar to that of ebR, this substitution did substantially alter the photocycle kinetics. The lifetime of the 570-nm absorbance change was increased over 10-fold, while the lifetime of the 410-nm absorbance change due to the M intermediate was only increased by about 20%. The 410-nm absorbance change for P186G was well fit by a single exponential, while the absorbance change at 570 nm clearly had a fast and a slow component.

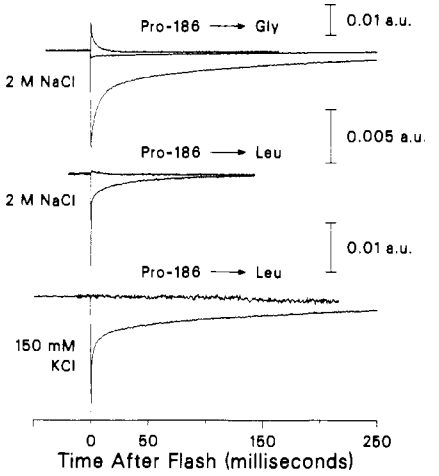

FIGURE 5: Absorbance changes for P186G and P186L. Absorbance changes are shown at 570, 410, and 640 nm for P186G in 2 M NaCl (0.55) and at 570 and 410 nm for P186L in 2 M NaCl (0.73) and in 0.15 M KCl (0.07). The absorbance of each sample at 570 nm is shown in parentheses. Since the λ_{max} of P186L in 0.15 M KCl was shifted to 470 nm, the 570-nm absorbance for this sample was relatively low. The amplitude of the 410-nm change was significantly reduced for P186L in 2 M NaCl, while there was no positive 410-nm absorbance change for P186L in 0.15 M KCl. All the record sets are displayed on the same time scale, which is shown below. The P186G and P186L records in 2 M NaCl are for 32 °C, while the P186L in 0.15 M KCl is at 25 °C.

Discussion

In this paper, we have examined the effects of eight single amino acid substitutions in helix F on the bR photocycle. Comparison of the photocycle kinetics of the eight mutants revealed four distinct groups. Table IV lists three characteristics we have used to separate the mutant photocycles into these four groups. The ratio $-\Delta A_{570}/A_{570}$ is a measure of the photocycle amplitude normalized to the amount of bR in the sample as measured by the 570-nm absorbance of the sample. The amount of M intermediate formed normalized to the amplitude of the photocycle is estimated by the $-\Delta A_{410}/\Delta A_{570}$ ratio. The ratio τ_{570}/τ_{410} indicates how closely the M intermediate decay is correlated with the lifetime of the photocycle measured at 570 nm.

Group A comprised the mutants S183A and E194Q. The photocycle characteristics of this group were qualitatively the most similar to those of the ebR and PM photocycles. The normalized amplitudes of transient absorbance changes ($-\Delta A_{570}/A_{570}$) of the Trp mutants W182F and W189F, i.e., group B, were significantly smaller than those of the controls or group A. Group C, which consisted of Y185F and S193A, was characterized by a large increase in the lifetime of the 570-nm absorbance change relative to the 410-nm absorbance

change, i.e., a higher value for τ_{570}/τ_{410}. These amino acid substitutions that removed hydrogen-bonding side-chain groups did not eliminate the photocycle or proton pumping (Hackett et al., 1987). This indicates that none of these residues are essential elements in a single-proton conduction pathway or wire. The substitutions at Pro-186, which comprise group D, had the most pronounced effect on the photocycle kinetics. How each of these individual amino acid substitutions affected the bR photocycle is discussed below.

Ser-183 and Glu-194. The amino acid substitutions at these residues did not significantly alter proton pumping (Hackett et al., 1987) or the UV/visible difference spectra of the K and M intermediates (Ahl et al., 1988). Although the Glu-194→Gln photocycle kinetics were slightly slower than those of the ebR case, these substitutions clearly produced the smallest alterations to the photocycle among the helix F mutants we examined. This indicates that these residues do not appear to be directly involved in the molecular mechanism of the photocycle and are unlikely to directly interact with the chromophore. A helical wheel projection analysis (Schiffer & Edmundson, 1967) of helix F (Figure 1) shows that these residues fall outside the cluster formed by the other mutants.

Trp-182 and Trp-189. As shown in Table IV, substitutions at Trp-182 and Trp-189 reduced the relative amplitudes of the absorbance change at 570 nm by approximately 10-fold compared to ebR and PM, without producing substantial changes in the other photocycle characteristics. These substitutions also reduced the amplitudes of the low-temperature BR→K UV/visible and FTIR difference spectra peaks, but did not significantly shift the λ_{max} of the major photocycle intermediates (Ahl et al., 1988; Rothschild et al., 1989a). Such effects are consistent with the hypothesis that Trp-182 and Trp-189 are positioned close to the retinal (Rothschild et al., 1989a,b). In this model, these amino acids constrain the motions of retinal during photoisomerization and restrict the possible configurations of retinal in the retinal-binding pocket of light-adapted bR. Replacement of either of these residues by Phe would relax these constraints. This could lead to the formation of species of BR that do not initiate the photocycle efficiently or have altered photocycles.

Tyr-185. The Tyr-185→Phe substitution had an unusual effect of significantly increasing the lifetime of the photocycle at 570 nm while not producing a corresponding increase in the lifetime of the M intermediate at 410 nm. In contrast, most agents that slow the overall photocycle, such as guanidine hydrochloride (Yoshida et al., 1977), glutaraldehyde (Ahl & Cone, 1984), and La^{3+} (Chang et al., 1986), increase the lifetime of the both the 570- and 410-nm absorbance changes to approximately the same degree. In addition, mutations at Asp-96, Asp-115, and Asp-212 also increase both the lifetime of the M intermediate and the lifetime of the 570-nm absorbance change (Holz et al., 1989; Stern et al., 1989). These agents and mutations increase the lifetime of the photocycle by apparently stabilizing the M intermediate. The increase in the photocycle lifetime of Y185F, however, does not result from slowing the decay of the M intermediate.

One explanation for the unusual Y185F photocycle is that there exist two distinct forms of this mutant which have different photocycles. One form would have an M intermediate with relatively normal photocycle kinetics near 570 nm. The other Y185F photocycle would be abnormal, having a slow absorbance change at 570 nm and no M-like intermediate. This hypothesis is supported by recent flash photolysis measurements using an optical multichannel analyzer, which indicates that there are at least two forms of Y185F. One form has a λ_{max} near 550 nm, while the λ_{max} of the other form is red-shifted to around 600 nm and has a photocycle similar to deionized blue membrane (M. Duñach, S. Berkowitz, T. Marti, T. Mogi, H. G. Khorana, and K. J. Rothschild, unpublished results). Flash studies using a variable-wavelength excitation also support this conclusion (D.-J. Jong, M. A. El-Sayed, L. J. Stern, T. Mogi, and H. G. Khorana, unpublished results).

Ser-193. The Ser-193→Ala substitution reduced the amplitude of the photocycle similar to W182F and W189F and also increased the τ_{570}/τ_{410} ratio like Y185F. These effects suggest that Ser-193 influences the interaction of Trp-182, Trp-189, and Tyr-185 with retinal. A helical wheel projection plot of the helix F indicates Ser-193 would be located within a 100° segment together with these residues. Ser-193 may provide an important hydrogen bond that helps to maintain the proper orientation of these residues relative to the chromophore.

Pro-186. Our results indicate that Pro-186 is essential for normal function of the photocycle. The Pro-186→Leu substitution blocks the formation of the M intermediate at 0.15 M KCl. At 2 M NaCl this substitution significantly inhibits the formation of the M intermediate. None of the other helix F mutants we examined blocked the formation of the M intermediate. The only other mutations that are known to block M formation are the Asp-85→Asn and Asp-212→Asn substitutions (Stern et al., 1989).

There are several possible roles for the Pro-186 in the photocycle. Since Pro-186 is believed to comprise part of the retinal-binding pocket, substitutions such as Leu might interfere with the proper fit of retinal (Ahl et al., 1988; K. J. Rothschild, Y.-W. He, T. Mogi, T. Marti, L. J. Stern, and H. G. Khorana, unpublished results). Alternatively, the proximity of Pro-186 to Tyr-185 suggests that this residue might be somehow affecting the observed changes of Tyr-185. In fact, recent FTIR studies on bR Pro mutants confirm that substitutions at Pro-186 do affect Tyr-185 (K. J. Rothschild, Y.-W. He, T. Mogi, T. Marti, L. J. Stern, and H. G. Khorana, unpublished results). It is possible that Pro-186 undergoes a conformational change during the photocycle which is required for normal proton pumping.

SUMMARY

We have combined flash spectroscopy techniques and site-specific mutagenesis to examine the role of specific residues in helix F of bacteriorhodopsin. Our results are consistent with the following model:

(i) Trp-182, Tyr-185, Pro-186, Trp-189, and Ser-193 form part of the binding pocket for retinal, while Ser-183 and Glu-194 are directed away from the retinal-binding site. Substitutions at Trp-182, Tyr-185, Pro-186, Trp-189, and Ser-193 all significantly affected the photocycle kinetics. In contrast, the photocycle perturbations produced by substitutions at Ser-183 and Glu-194 were relatively small.

(ii) Trp-182 and Trp-189 interact with the chromophore. Substitutions at these positions significantly decresaed the amplitude of the photocycle. These residues may sterically constrain retinal during photoexcitation.

(iii) Pro-186 is important for maintaining the protein structure around the chromophore. The Pro-186→Gly substitution produced large alterations in the photocycle kinetics, while the Pro-186→Leu substitution inhibited the formation of the M intermediate.

(iv) Tyr-185 plays a role in the overall photocycle, possibly through photocycle protonation changes proposed by Braiman et al. (1988a). A substitution of this Tyr by a Phe results in a large alteration in the photocycle. This substitution may

produce two different Y185F photocycles.

ACKNOWLEDGMENTS

We thank M. S. Braiman, P. Roepe, M. Duñach, C. Montague, S. Subramaniam, and M. Heyn for many helpful discussions during the course of this work.

Registry No. Ser, 56-45-1; Glu, 56-86-0; Tyr, 60-18-4; Pro, 147-85-3; Trp, 73-22-3.

REFERENCES

Ackers, G. K., & Smith, R. F. (1985) *Annu. Rev. Biochem. 54*, 597–629.

Ahl, P. L., & Cone, R. A. (1984) *Biophys. J. 45*, 1039–1049.

Ahl, P. L., Stern, L. J., Düring, D., Mogi, T., Khorana, H. G., & Rothschild, K. J. (1988) *J. Biol. Chem. 263*, 13594–13601.

Bayley, H., Huang, K.-S., Radhakrishnan, R., Ross, A. H., Takagaki, Y., & Khorana, H. G. (1981) *Proc. Natl. Acad. Sci. U.S.A. 78*, 2225–2229.

Bayley, H., Hojeberg, B., Huang, K.-S., Khorana, H. G., Liao, M.-J., Lind, C., & London, E. (1982) *Methods Enzymol. 88*, 74–81.

Bevington, P. R. (1969) *Data Reduction and Error Analysis for the Physical Sciences*, McGraw-Hill, New York.

Braiman, M., & Mathies, R. (1982) *Proc. Natl. Acad. Sci. U.S.A. 79*, 403–407.

Braiman, M. S., Stern, L. J., Chao, B. H., & Khorana, H. G. (1987) *J. Biol. Chem. 262*, 9271–9276.

Braiman, M. S., Mogi, T., Stern, L. J., Hackett, N., Chao, B. H., Khorana, H. G., & Rothschild, K. J. (1988a) *Proteins: Struct., Funct., Genet. 3*, 219–229.

Braiman, M. S., Mogi, T., Marti, T., Stern, L. J., Khorana, H. G., & Rothschild, K. J. (1988b) *Biochemistry 27*, 8516–8520.

Chang, C. H., Jonas, R., Melchiore, S., Govindjee, R., & Ebrey, T. G. (1986) *Biophys. J. 49*, 731–739.

Dancsházy, Z. S., Govindjee, R., & Ebrey, T. G. (1988) *Proc. Natl. Acad. Sci. U.S.A. 85*, 6358–6361.

Hackett, N. R., Stern, L. J., Chao, B. H., Kronis, K. A., & Khorana, H. G. (1987) *J. Biol. Chem. 262*, 9277–9284.

Henderson, R., & Unwin, P. N. T. (1975) *Nature (London) 275*, 28–37.

Holz, M., Drachev, L. A., Mogi, T., Otto, H., Kaulen, A. D., Heyn, M. P., Skulachev, V. P., & Khorana, H. G. (1989) *Proc. Natl. Acad. Sci. U.S.A. 86*, 2167–2171.

Huang, K.-S., Radhakrishnan, R., Bayley, H., & Khorana, H. G. (1982) *J. Biol. Chem. 257*, 13616–13623.

Katre, N. V., Wolber, P. K., Stoeckenius, W., & Stroud, R. M. (1981) *Proc. Natl. Acad. Sci. U.S.A. 78*, 4068–4072.

Khorana, H. G., Gerber, G. E., Herlihy, W. C., Gray, C. P., Anderegg, R. J., Nihei, K., & Biemann, K. (1979) *Proc. Natl. Acad. Sci. U.S.A. 76*, 5046–5050.

Knowles, J. R. (1987) *Science 236*, 1252–1258.

Kouyama, T., Nasuda-Kouyama, A., Ikegami, A., Mathew, M. K., & Stoeckenius, W. (1988) *Biochemistry 27*, 5855–5863.

Lo, K.-M., Jones, S. S., Hackett, N. R., & Khorana, H. G. (1984) *Proc. Natl. Acad. Sci. U.S.A. 81*, 2285–2289.

Lozier, R. H., Bogomolni, R. A., & Stoeckenius, W. (1975) *Biophys. J. 15*, 955–962.

Mogi, T., Stern, L. J., Hackett, N. R., & Khorana, H. G. (1987) *Proc. Natl. Acad. Sci. U.S.A. 84*, 5595–5599.

Mogi, T., Stern, L. J., Marti, T., Chao, B. H., & Khorana, H. G. (1989a) *J. Biol. Chem. 264*, 14192–14196.

Mogi, T., Marti, T., & Khorana, H. G. (1989b) *J. Biol. Chem. 264*, 14197–14201.

Nagle, J. F., & Morowitz, H. J. (1978) *Proc. Natl. Acad. Sci. U.S.A. 75*, 298–302.

Nagle, J. F., Parodi, L. A., & Lozier, R. H. (1982) *Biophys. J. 38*, 161–174.

Oesterhelt, D., & Stoeckenius, W. (1974) *Methods Enzymol. 31*, 667–678.

Ovchinnikov, Y. A., Abdulaev, N. G., Feigina, M. Y., Kiselev, A. V., & Lobanov, N. A. (1979) *FEBS Lett. 100*, 219–224.

Popot, J.-L., Trewhella, J., & Engelman, D. M. (1986) *EMBO J. 5*, 3039–3044.

Rothschild, K. J., Argade, P. V., Earnest, T. N., Huang, K.-S., London, E., Liao, M.-J., Bayley, H., Khorana, H. G., & Herzfeld, J. (1982) *J. Biol. Chem. 257*, 8592–8595.

Rothschild, K. J., Gray, D., Mogi, T., Marti, T., Braiman, M. S., Stern, L. J., & Khorana, H. G. (1989a) *Biochemistry 28*, 7052–7059.

Rothschild, K. J., Braiman, M. S., Mogi, T., Stern, L. J., & Khorana, H. G. (1989b) *FEBS Lett. 250*, 448–452.

Schiffer, M., & Edmundson, A. B. (1967) *Biophys. J. 7*, 121–135.

Stern, L. J., Ahl, P. L., Marti, T., Mogi, T., Duñach, M., Berkowitz, S., Rothschild, K. J., & Khorana, H. G. (1989) *Biochemistry* (following paper in this issue).

Trewhella, J., Popot, J.-L., Zaccai, G., & Engelman, D. M. (1986) *EMBO J. 5*, 3045–3049.

Xie, A. H., Nagle, J. F., & Lozier, R. H. (1987) *Biophys. J. 51*, 627–635.

Yoshida, M., Ohno, K., Takeuchi, Y., & Kagawa, Y. (1977) *Biochem. Biophys. Res. Commun. 75*, 1111–1116.